

USING IMS IS-13 AND IS-14 STATIONS TO ANALYZE STRONG SEISMIC AND VOLCANIC ACTIVITY IN CHILE



Rodrigo De Negri¹, Paola García² & Jaime Campos¹

(1) Department of Geophysics, University of Chile, (2) Chilean Nuclear Energy Commission, Santiago, Chile

Please write me at:
rdenegri@dgf.uchile.cl
or
rodenegri@gmail.com

T1.1-P24

1. Introduction

Since 2004, IMS infrasound arrays IS-13 and IS-14, located at Easter Island and Robinson Crusoe Island (Chile), respectively, have been recording continuously through some of the most energetic eruptions and earthquakes in recent history in the country. Infrasound fingerprint, though, has been scarcely studied using this data.

Because of this we have started a long term project between University of Chile and the Chilean Nuclear Energy Commission (CCHEN), which holds the National Data Center of CTBT, to make scientific use of these data. As a first experiment we have collected the data around three strong infrasound generating events: (i) M8.8 Maule tsunamigenic earthquake on 27 February 2010, (ii) Puyehue/Cordón Caulle volcano eruption in June 2011 and (iii) Calbuco volcano eruption in April 2015. Using some of the tools provided by the Data Center, we have been able to recover some interesting information about the processes involved.

2. Stations IS13 and IS14

Arrays I-13 and I-14 are located at global distances (> 250 km distance) from Chilean territory. Both are composed of eight MB2000 microbarometers, with two mini arrays to ensure optimised low and high frequency ranges for detections.

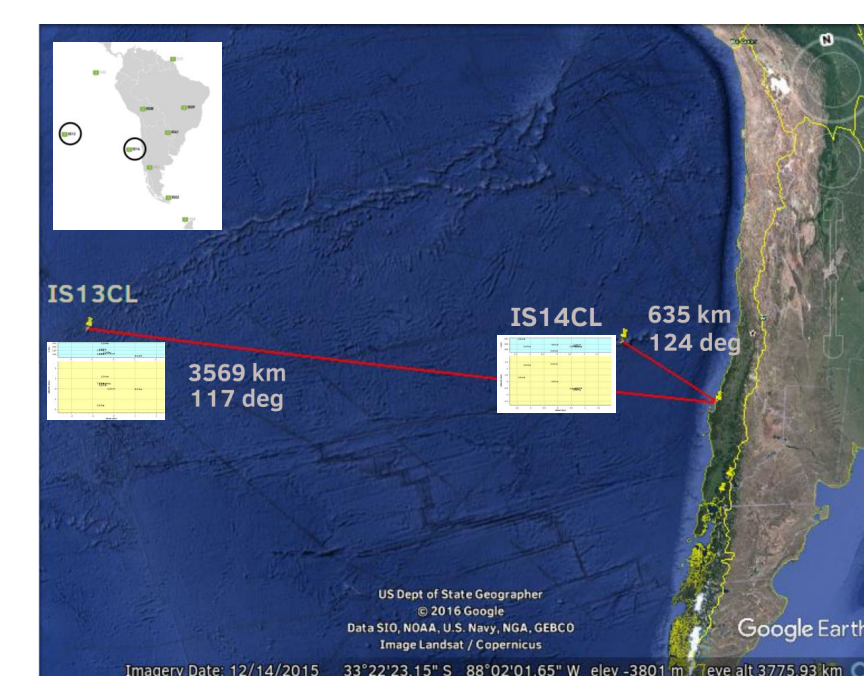


Fig. 1: Distances and azimuths from stations to Maule's earthquake zone (2010).

3. The earthquake of Maule

On 27 February 2010, a M8.8 earthquake occurred in the coast of the Maule Region, Chile at 06:34:14 UTC, with a focal depth 30.1 km, and a rupture length about 500 km. The rupture propagated mainly from south to north.

Figure 2 shows GPS results for vertical static displacement that could cause a considerable vertical air-ground coupling movement, releasing infrasound waves to the atmosphere.

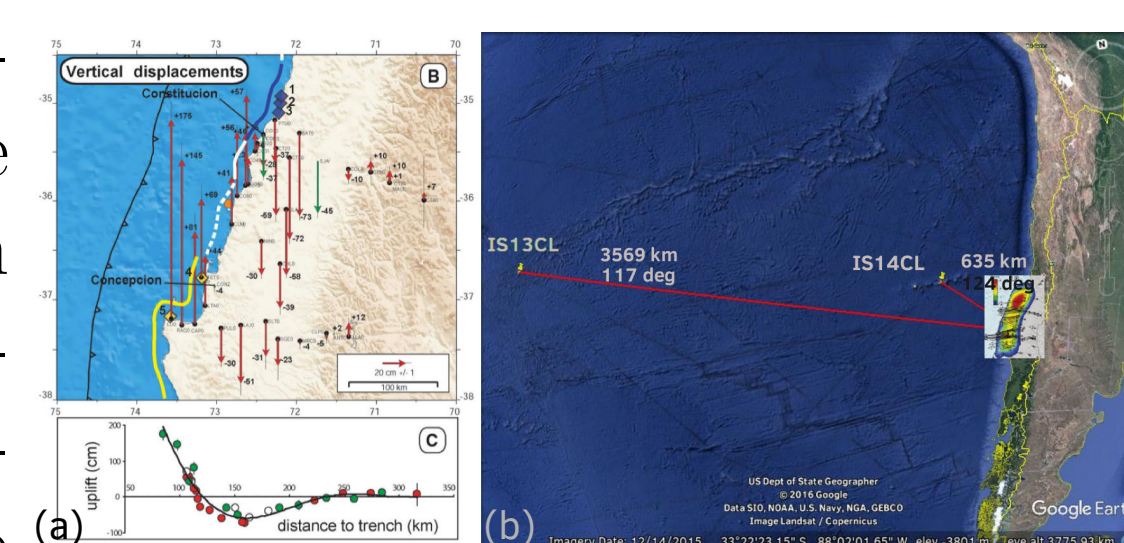


Fig. 2: (a) Vertical component of coseismic static displacement field (red arrows) and cGPS sites (green arrows) in the epicentral area (Vigny et al., 2011) (b) Rupture area scaled with the continent.

4. Calbuco eruption

On 22 April 2015 at 18:04 UTC Calbuco volcano, after more than 40 years of resting, started a VEI-4 eruption with a big explosive event that sent an ash plume 15 km above the crater. Precursory activity was scarce, with about 2-3 hours of increased seismicity, surprising authorities and scientific community. The first two and strongest phases, with sustained ash plumes of 15 km of height, probably generated jet-noise type of infrasound.

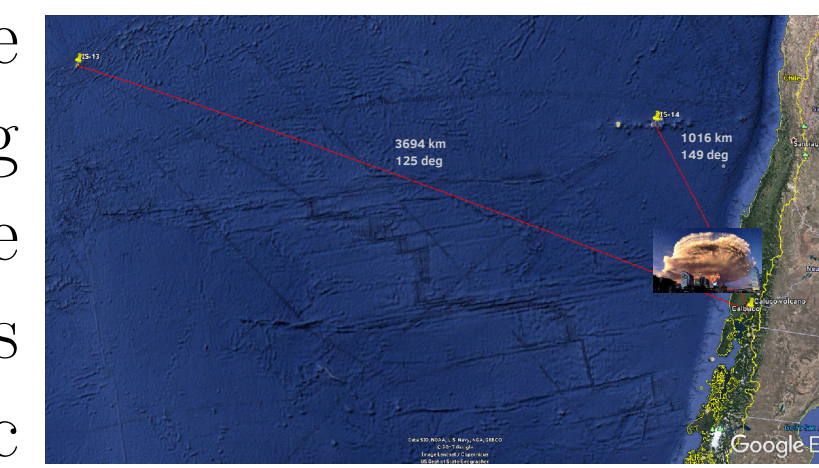


Fig. 3: Infrasound stations to Calbuco volcano location as a reference.

5a. Earthquake results

The following results were obtained using the version 5.5 of the interactive tool DTK-GPMCC, provided by the National Data Center of the CTBT Project.

Figures 4 and 5 show that infrasound detections of epicenter-generated waves on February 27 can be seen for both arrays. For IS-14 array, time range is abruptly cut in the moment in which the Tsunami waves destroyed the communication system.

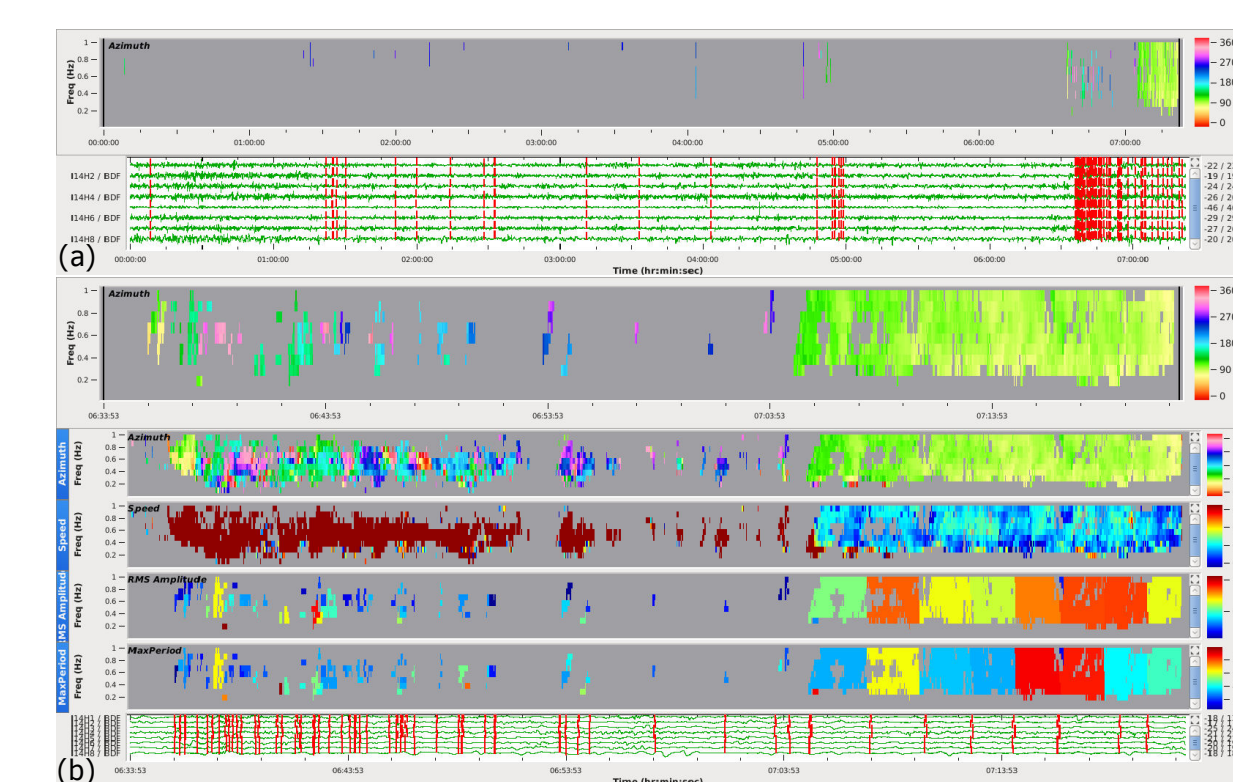


Fig. 4: Detections for IS-14. (a) The "complete" time window. (b) Zoom around expected infrasonic detections.

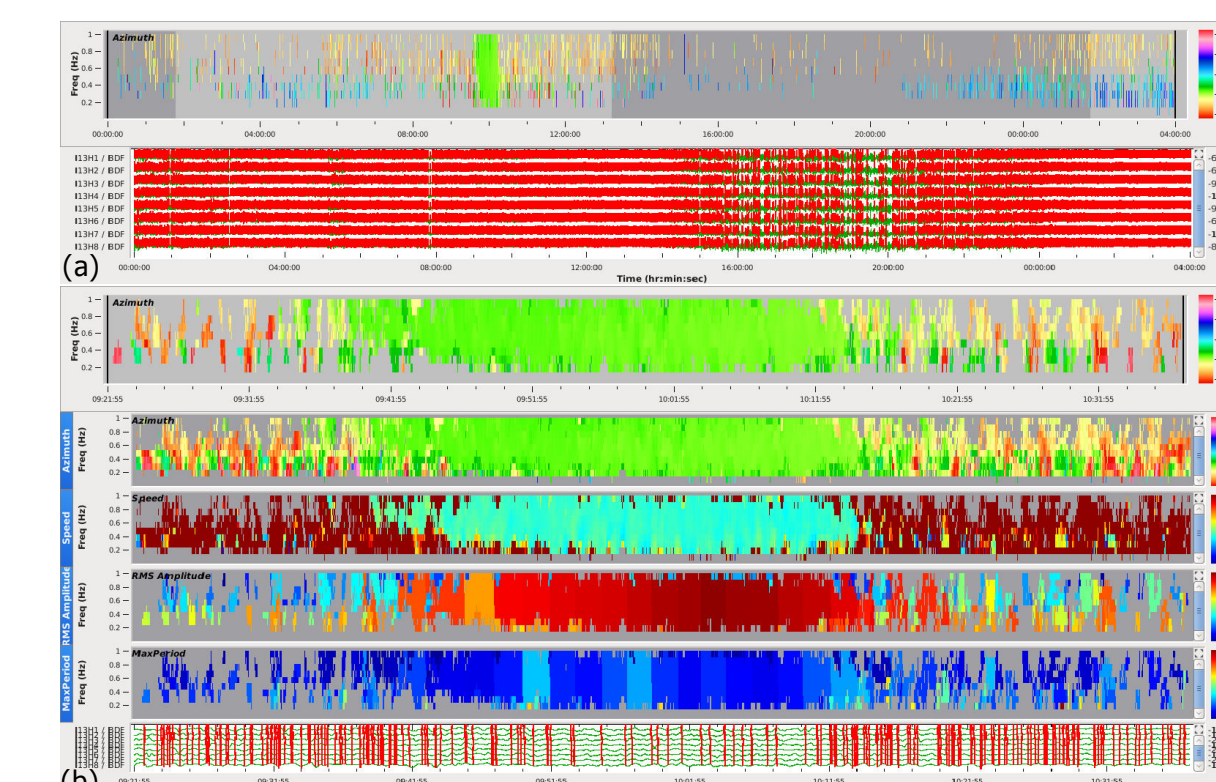


Fig. 5: Detections for IS-13. (a) The complete time window. (b) Zoom around expected infrasonic detections.

Figures 6 and 7 show polar plots in azimuth for RMS amplitudes and speed in time. Both parameters allow us to see how the superficial source propagated in N-S direction, specially when detections are plotted as families.

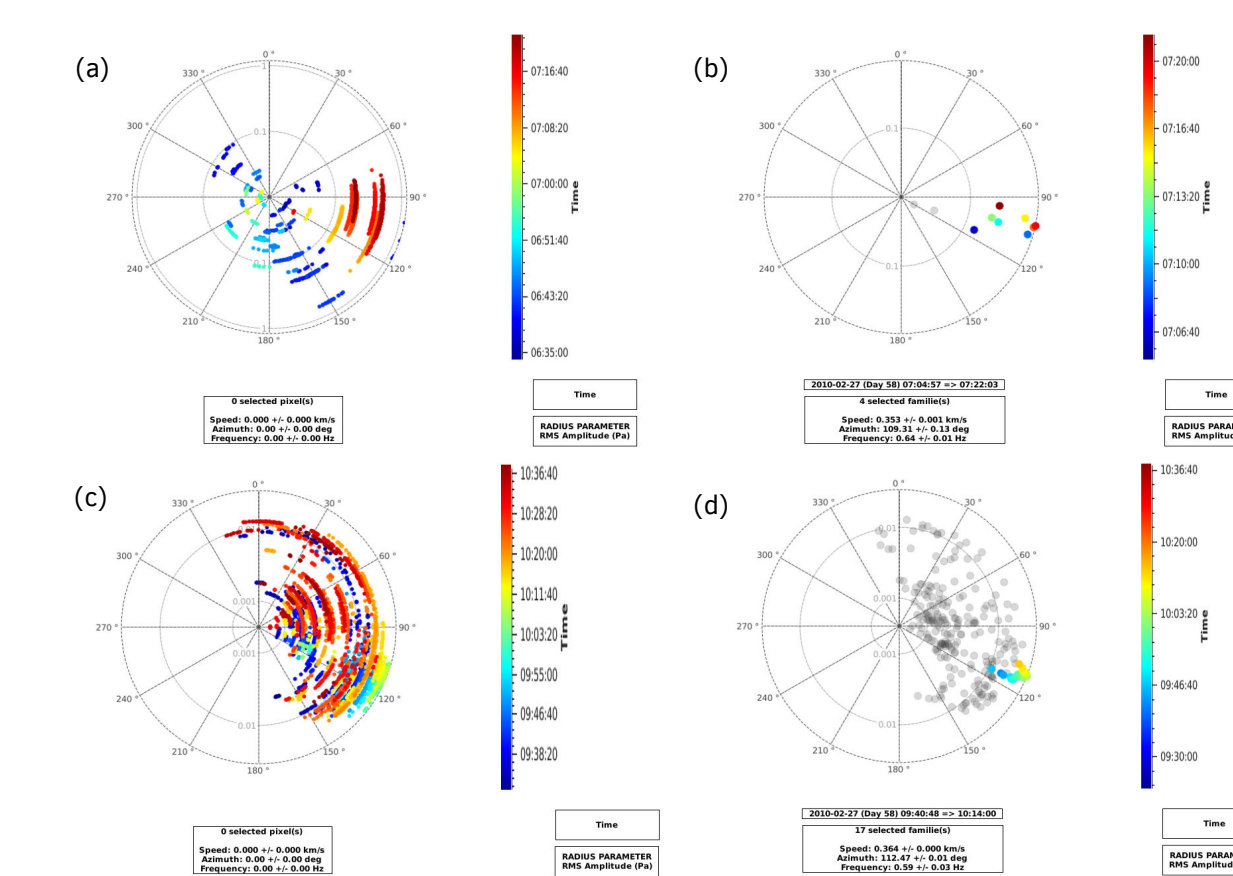


Fig. 6: Polar plots in azimuth of RMS amplitude in time. (a) and (c): all detections for IS-14 and IS-13, respectively. (b) and (d): family detections for IS-14 and IS-13, respectively.

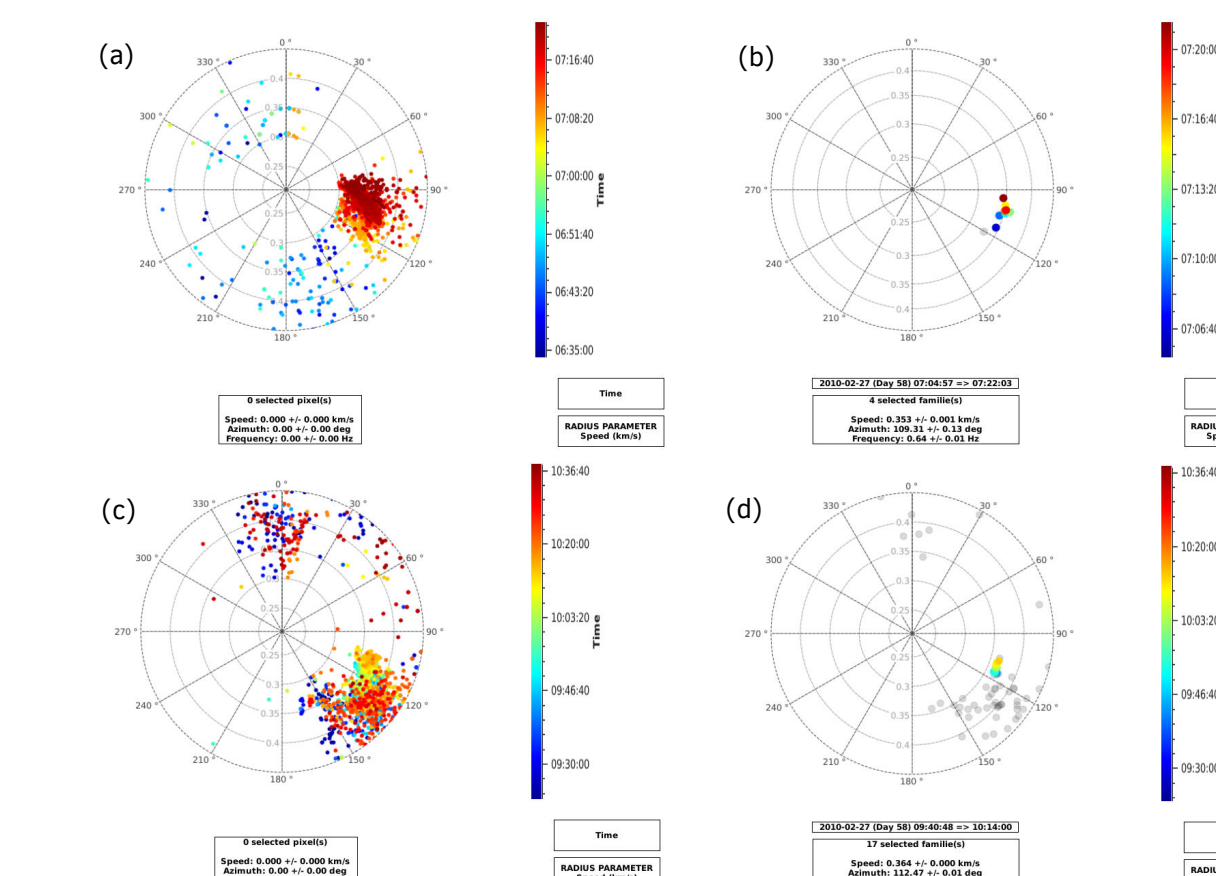


Fig. 7: Polar plots in azimuth of speed in time. (a) and (c): all detections for IS-14 and IS-13, respectively. (b) and (d): family detections for IS-14 and IS-13, respectively.

5b. Calbuco eruption results

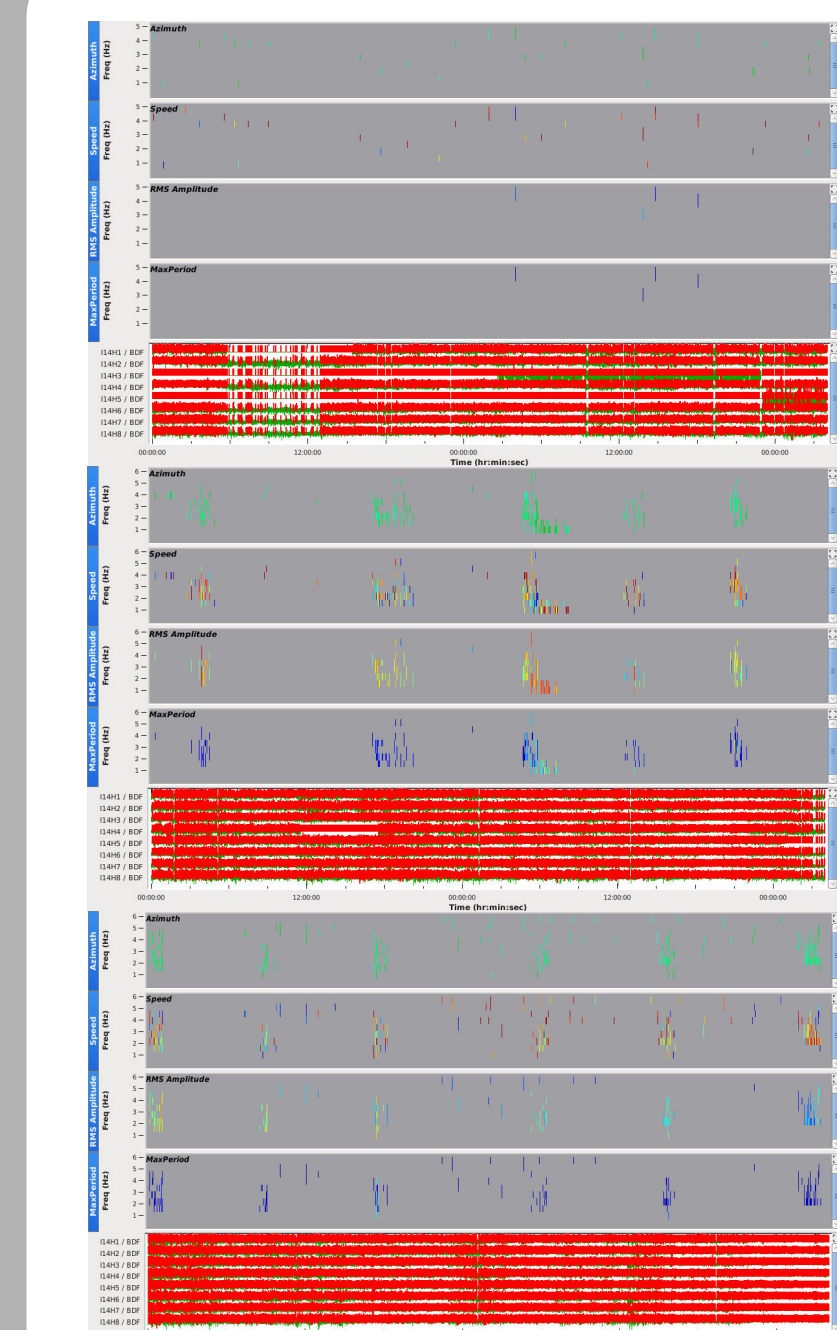


Fig. 8: Detections (left) and polar plots (right) for IS-14 array. 0.5 to 6.0 Hz. (a) 19-21 April. (b) 22-24 April. (c) 03-05 May. There is sustained episodic activity after the most active phases which are not correlated with any sustained ash column observed.

Figure 9 shows two detection sequences for the array I-13 (~ 3700 km): before and during the most active phase of the eruption. Only the IVLP band showed relevant information for all the different days calculated, probably because of the low attenuation for this frequency band when compared to the other two. The lack of detections in this band for I-14 array suggest that there is a shadow zone effect present.

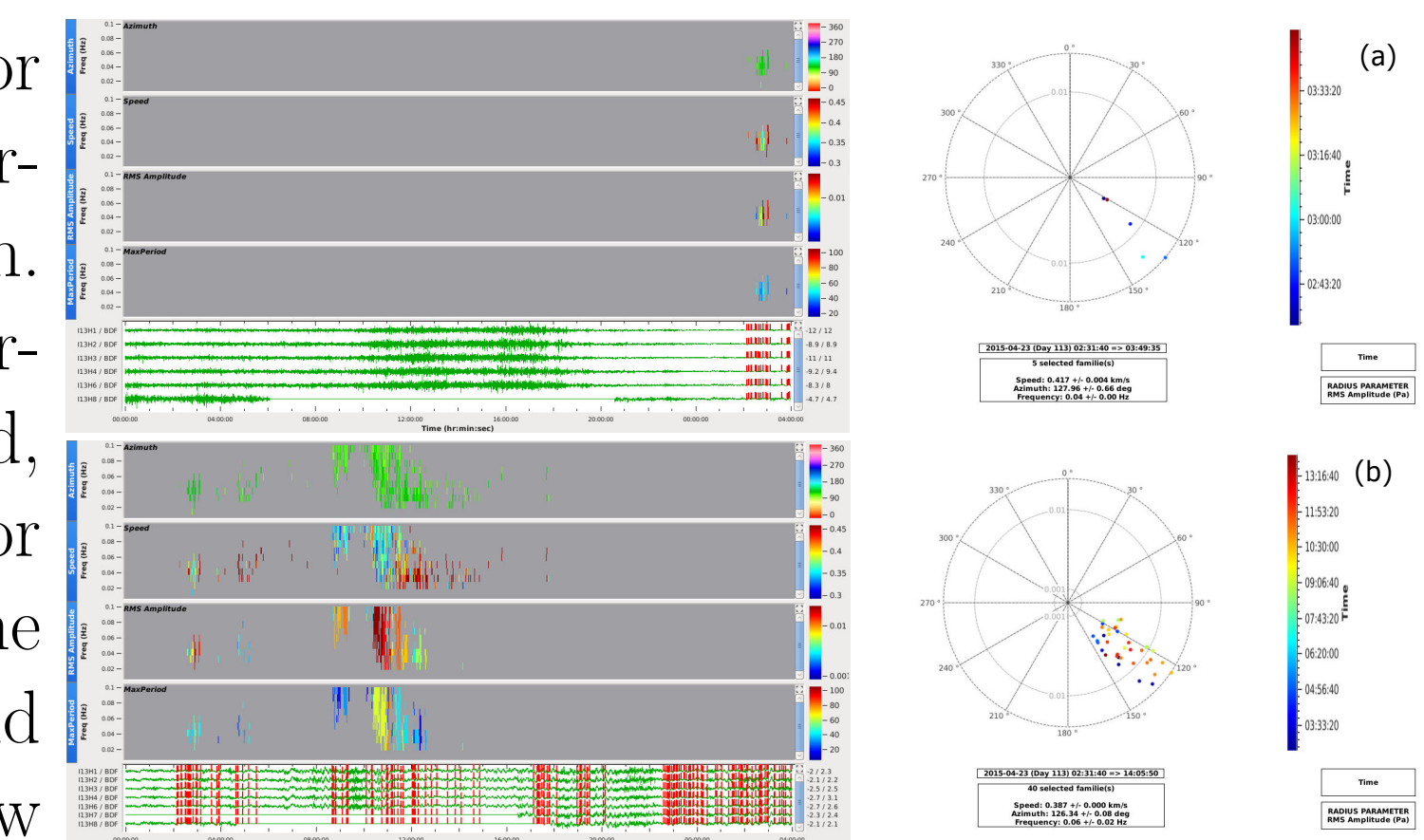


Fig. 9: Detections (left) and polar plots (right) for IS-13 array. 0.01 to 0.1 Hz. (a) 22-23 April. (b) 23-24 April.

6. Remarks and future work

Results around Calbuco eruption show that for sustained strong ash plume activity, detections in the expected frequency bands, azimuths and times can be achieved for both arrays. For IS-14 array, we see sustained episodic infrasound detections from the expected azimuth even several days after the strong phase of the eruption in the MP and SP frequency bands. This detections do not resemble normal previous activity, suggesting that there is another type of activity that is worth to analyze. For IS-13 array only the IVLP band shows detections that can be related with Calbuco eruption. IS-14 fails to detect activity in this band, suggesting that it might be situated over a shadow zone.

For the earthquake of Maule, we could detect infrasound in a wider frequency band, and localize the "infrasound" epicenter in azimuth and time. We also see that earthquakes along the seismogenic zone of encounter between Nazca and Sudamerican Plates can be detected and studied using IS-13 and IS-14 arrays.

Future work could be centered in using atmospheric models to have a better understanding of the infrasound generation and propagation. To consider seismic and satelital data to complement detection and characterization of large earthquakes and eruptions is certainly a task to complete. Having a third array located at local (< 100 km) distance of some zones of interest, could improve infrasound characterization and also diminish the latency of infrasound detections to detect high ash clouds and improve hazard assessment.

References

- [1] Kenneth M. Arnoult et al. "Infrasound observations of the 2008 explosive eruptions of Okmok and Kasatochi volcanoes, Alaska". In: *JGRA* 115.20 (2010), pp. 1–12.
- [2] Y Cansi and Alexis Le Pichon. "Infrasound Event Detection Using the Progressive Correlation Algorithm". In: *SPA* (2008), pp. 1425–1435.
- [3] David Fee, Milton Garces, and Andrea Steffke. "Infrasound from Tungurahua Volcano 2006–2008: Strombolian to Plinian eruptive activity". In: *JVGR* 193.1-2 (2010), pp. 67–81.
- [4] David Fee, Andrea Steffke, and Milton Garces. "Characterization of the 2008 Kasatochi and Okmok eruptions using remote infrasound arrays". In: *JGRA* 115.18 (2010), pp. 1–15.
- [5] David Fee et al. "Combining local and remote infrasound recordings from the 2009 Redoubt Volcano eruption". In: *JVGR* 259 (2013), pp. 100–114.
- [6] Andrea M. Steffke et al. "Eruption chronologies, plume heights and eruption styles at Tungurahua Volcano: Integrating remote sensing techniques and infrasound". In: *JVGR* 193.3-4 (2010), pp. 143–160.
- [7] Alexa R. Van Eaton et al. "Volcanic lightning and plume behavior reveal evolving hazards during the April 2015 eruption of Calbuco volcano, Chile". In: *GRL* 43.7 (2016), pp. 3563–3571.
- [8] C. Vigny. "The 2010 Mw 8.8 Maule Megathrust Earthquake of Central Chile, Monitored by GPS". In: *Science* 332 (2011).